

JAAS

Accepted Manuscript



This is an *Accepted Manuscript*, which has been through the Royal Society of Chemistry peer review process and has been accepted for publication.

Accepted Manuscripts are published online shortly after acceptance, before technical editing, formatting and proof reading. Using this free service, authors can make their results available to the community, in citable form, before we publish the edited article. We will replace this *Accepted Manuscript* with the edited and formatted *Advance Article* as soon as it is available.

You can find more information about *Accepted Manuscripts* in the [Information for Authors](#).

Please note that technical editing may introduce minor changes to the text and/or graphics, which may alter content. The journal's standard [Terms & Conditions](#) and the [Ethical guidelines](#) still apply. In no event shall the Royal Society of Chemistry be held responsible for any errors or omissions in this *Accepted Manuscript* or any consequences arising from the use of any information it contains.

1
2
3 1 **Application of disposable starch-based platforms for sample**
4
5 2 **introduction and determination of refractory elements using graphite**
6
7 3 **furnace atomic absorption spectrometry and direct solid sample**
8
9 4 **analysis**
10
11
12
13
14

15 6 *Lígia Colares, Éderson R. Pereira, Josias Merib, Julyetty C. Silva, Jaqueline M. Silva,*
16

17 7 *Bernhard Welz, * Eduardo Carasek, Daniel L.G. Borges*

18 8 Departamento de Química, Universidade Federal de Santa Catarina, 88040-900
19

20 9 Florianópolis, SC, Brazil
21
22
23

24 10
25
26 11 *Corresponding Author, e-mail address: w.bernardo@terra.com.br (B. Welz).
27

28 12 FAX: +55 48 3721 6850
29
30
31 13
32
33
34
35
36
37
38
39
40
41
42
43
44
45
46
47
48
49
50
51
52
53
54
55
56
57
58
59
60

1
2
3 14 **Abstract**
4
5

6 15 This study describes a new approach for direct solid sample analysis using
7
8 16 thermoplastic starch (TPS) platforms for the determination of Mo and V by high-
9
10 17 resolution continuum source graphite furnace atomic absorption spectrometry (HR-CS
11
12 18 GF AAS). The TPS platform was prepared from a mixture of commercial corn starch
13
14 19 (28% amylase and 72% amylopectin), with sorbitol as plasticizer in a 70/30 mass-based
15
16 20 ratio. Different parameters affecting the film composition, such as proportion and
17
18 21 plasticizer type, were evaluated taking into account the behavior in the graphite tube
19
20 22 when the TPS platform was subjected to the heating program. The new sample
21
22 23 introduction approach has been shown to increase the graphite tube lifetime
23
24 24 significantly due to a much less pronounced tailing of the absorbance signals of
25
26 25 elements such as Mo or V, which makes possible reducing atomization and cleaning
27
28 26 times, compared to the use of a conventional graphite platform. Memory effects were
29
30 27 significantly reduced using the starch-based platform, resulting in improved precision.
31
32 28 Detection limit and characteristic mass were determined as 25 pg and 7 pg for Mo, and
33
34 29 130 pg and 18 pg for V, respectively. The accuracy was confirmed by the analysis of a
35
36 30 series of certified reference materials, including bovine liver, beef liver, rice flour and
37
38 31 urban dust for Mo, and coal, urban dust, lichen and particulate matter for V,
39
40 32 respectively.
41
42
43
44
45
46
47
48
49
50

51 33 *Keywords:* Direct solid sample analysis; Graphite furnace AAS; Thermoplastic starch
52
53 34 platform; Molybdenum determination; Vanadium determination.
54
55
56
57
58
59
60

1
2
3 364
5 37 **1. Introduction**

6
7
8 38 Elemental analysis using graphite furnace atomic absorption spectrometry (GF AAS)
9
10 39 involves well-established procedures, although handling and preparation of solid
11
12 40 samples for analysis are still regarded as critical stages of an analytical method. Usually,
13
14 41 solid samples are brought into solution using 'classical' procedures, which might
15
16 42 include dry ashing,¹ alkaline fusion^{2,3} or oxidative acid digestion.⁴⁻⁶ Despite the
17
18 43 favorable characteristics inherent to each of these procedures, several limitations are
19
20 44 also associated to the analytical task of bringing a solid sample into a solution, which
21
22 45 depends on the sample, the analytes and their concentrations. Systematic errors due to
23
24 46 contamination by reagents or lab ware, or losses by volatilization are amongst the most
25
26 47 frequent issues, and may directly affect the accuracy and precision of the analytical
27
28 48 results. In this context, analyte determination based on the direct analysis of solid
29
30 49 samples (SS), which minimizes processing of the samples, appears as an interesting
31
32 50 alternative.^{7,8}

33
34
35
36
37 51 The direct determination of trace elements by SS-GF AAS usually involves the
38
39 52 analysis of a powdered sample with controlled particle size. The advantages of this
40
41 53 procedure include simplified pre-treatment of the sample, allowing a reduction of
42
43 54 preparation time and minimized risk of contamination or analyte loss due to reduced
44
45 55 reagent consumption and to the absence of thermal treatment of the samples, among
46
47 56 others.^{7,9,10}

48
49
50 57 Application of direct SS analysis to the determination of refractory elements may
51
52 58 have restrictions, which are mostly associated with the low atomization efficiency due
53
54 59 to the relatively high mass of the SS platform and the resulting slower heating rate and
55
56 60 lower final temperature compared to that of the tube wall. Elements, such as

1
2
3 61 molybdenum and vanadium are very stable, so that high atomization temperatures are
4
5 62 required, which significantly reduce the lifetime of graphite tubes and platforms. The
6
7 63 atomization efficiency would be higher for atomization from the wall; however, direct
8
9 64 SS analysis requires the use of graphite platforms for sample weighing and
10
11 65 transportation to the graphite furnace.¹¹ These aspects lead to the idea of using a
12
13 66 platform made of a thermally degradable material, such as starch, which would serve
14
15 67 simply as a sample holder to allow sample insertion into the graphite tube.
16
17

18
19 68 Starch is the main component of many grains, roots and tubers, such as corn, potato,
20
21 69 etc. and is a heterogeneous polysaccharide consisting of two polymers, amylose and
22
23 70 amylopectin, in variable proportions.^{12,13} Starch films tend to be inflexible and brittle,
24
25 71 but the addition of plasticizers, such as glycerol or sorbitol, leads to the formation of
26
27 72 thermoplastic starch (TPS), which has improved mechanical properties. These
28
29 73 polymeric films have acquired great importance, which is mostly due to the fact that
30
31 74 they might be used as a source of biodegradable materials, renewable sources, with
32
33 75 relatively low cost.¹⁴
34
35

36
37 76 The aim of this work was to develop and to evaluate a new concept for direct SS
38
39 77 introduction for GF AAS, consisting of the use of TPS as a "platform" for the
40
41 78 determination of Mo and V in solid samples. The results obtained using the new TPS
42
43 79 platforms were compared to those for conventional SS graphite platforms, and certified
44
45 80 reference materials (CRM) were analyzed to evaluate the accuracy and practical
46
47 81 applicability of the proposed technique.
48
49

50 51 82 **2. Experimental**

52 53 54 55 83 *2.1. Instrumentation* 56 57 58 59 60

1
2
3 84 All measurements were carried out using a contrAA 600 high-resolution continuum
4
5 85 source atomic absorption spectrometer (Analytik Jena AG, Jena, Germany) with a
6
7 86 transversely heated graphite tube atomizer. The instrument is equipped with a 300 W
8
9
10 87 xenon short-arc lamp, operating in a 'hot-spot' mode, as a continuous radiation source
11
12 88 from 189-900 nm; a high-resolution double monochromator, consisting of a prism pre-
13
14 89 monochromator, an echelle grating monochromator, and a charge-coupled device
15
16 90 (CCD) array detector, providing a spectral bandwidth per pixel of about 1.2 pm at 200
17
18 91 nm.

19
20
21 92 Pyrolytically coated graphite tubes without platform, but with a dosing hole
22
23 93 (Analytik Jena, Part No. 407-A81.011), were used in all experiments with aqueous
24
25 94 standards and direct SS analysis. The solid samples were weighed directly onto SS
26
27 95 platforms (Analytik Jena Part No. 407-152.023) or TPS films using an M2P
28
29 96 microbalance (Sartorius, Göttingen, Germany). A manual solid sampling system, SSA 6
30
31 97 (Analytik Jena), was used to transport and insert the SS platforms or TPS films into the
32
33 98 graphite tube. Argon 99.996% (Oxilar, Florianópolis, Brazil) was used as purge and
34
35 99 protective gas. The temperature program used for Mo and V determination is shown in
36
37
38 100 Table 1.

39
40
41 101 A T1440 ultrasonic bath (Unique, São Paulo, Brazil), operated at 40 kHz and 81 W,
42
43 102 was used for preparation of the TPS polymeric films.

44 45 46 47 103 *2.2. Reagents and reference materials*

48
49
50 104 Ultrapure water obtained from a Mega ROUP Mega purity system (Equisul, Pelotas,
51
52 105 Brazil) with a specific resistivity of 18 MΩ cm was used throughout for preparation of
53
54 106 calibration solutions. The aqueous standards were prepared by serial dilution of the
55
56 107 individual stock standard solutions of 1000 mg L⁻¹ Mo and V (Sigma-Aldrich,
57
58
59
60

1
2
3 108 Steinheim, Germany). Commercial corn starch (Maizena, Garanhuns, Pernambuco,
4
5 109 Brazil), sorbitol 99% (Vetec, Rio de Janeiro, Brazil) and glycerin (glycerol) 99.5%
6
7 110 (Vetec), were used as supplied to produce the polymeric films.

8
9
10 111 The certified references materials (CRM) NIST 1649a “Urban Dust”, NIST 1577b
11
12 112 “Bovine Liver”, NIST 1568a “Rice flour” (National Institute of Standards and
13
14 113 Technology, Gaithersburg, MD, USA) and NCS ZC 71001 “Beef Liver” (NCS, Beijing,
15
16 114 China) were used to verify the accuracy for Mo, and that of V was verified using BCR
17
18 115 No. 180 “Gas Coal” (Community Bureau of Reference, Brussels, Belgium), IAEA-336
19
20 116 “Lichen” (International Atomic Energy Agency, Vienna, Austria), NIST 1648a “Urban
21
22 117 Particulate Matter” and NIST 1649a “Urban Dust”.

23 24 25 26 27 118 *2.3. Preparation of TPS platforms*

28
29
30 119 Different starch and plasticizer proportions, as well as plasticizer types were studied
31
32 120 considering the TPS film characteristics according to its behavior during the heating
33
34 121 program. Plasticizers are added to improve the mechanical properties such as
35
36 122 malleability of the polymeric film, and must be compatible with the biopolymer.¹⁴
37
38 123 Glycerol and sorbitol are amongst the most suitable plasticizers for starch, and glycerol
39
40 124 usually provides more pronounced effects upon the malleability of starch-based
41
42 125 films.^{14,15} When produced in the laboratory, the starch is dispersed in water, a plasticizer
43
44 126 is added, and the ingredients are thoroughly mixed. During drying, the ingredients form
45
46 127 a uniform layer that gives rise to films.¹⁶

47
48
49
50 128 For preparation of TPS films, 0.5 or 1.0 g of starch were added into a 50 mL beaker,
51
52 129 followed by 15 mL of distilled water and 0.1 or 0.3 g of the plasticizer, which was
53
54 130 added to prevent the film from becoming brittle. The mixture was immersed in an
55
56 131 ultrasonic bath for 6 min in order to increase the homogeneity, and then kept under
57
58
59
60

1
2
3 132 magnetic stirring and heating to 55 °C for 35 min. Finally, the mixture was transferred
4
5 133 to a previously heated Petri dish and left to stand in a fume hood until complete
6
7 134 evaporation of the water. Afterwards, the TPS films were cut into fragments of 4 mm x
8
9 135 10 mm with stainless steel scissors, in order to acquire dimensions similar to a
10
11 136 conventional SS platform. The starch and plasticizer proportions were varied according
12
13 137 to the conditions shown in Table 2.

138 2.4. Mo and V determination by HR-CS SS-GF AAS using TPS platforms

139 Aliquots varying from 0.05 to 0.8 mg of each CRM were weighed on TPS or
140 graphite platforms and transferred to the graphite tube using the SSA 6 accessory. The
141 transfer of the two types of platforms is shown in Figs. 1A and 1B, and the position of
142 the TPS platform inside the graphite tube in Figs. 1C and 1D. The TPS platform is
143 disintegrating during the first pyrolysis stage of the temperature program shown in
144 Table 1, leaving the sample directly on the tube wall. The main resonance lines at
145 313.259 nm for Mo and 318.398 nm for V were used, and the integrated absorbance
146 summated over three pixels around the line core ($A_{\Sigma 3, \text{int}}$) was used for signal evaluation.
147 Aqueous standard solutions were used for calibration for both elements, and calibration
148 solutions were pipetted directly onto the graphite tube wall in 20 μL aliquots.

149 3. Results and Discussion

150 3.1 Evaluation of the TPS platforms

151 A polymeric film made from a biopolymer is for the first time reported in this work
152 as a replacement material for the graphite platforms used in SS-GF AAS. One of the
153 main advantages associated to the use of a polymeric platform for refractory elements

1
2
3 154 resides in the fact that the platform readily decomposes in the pyrolysis stage, leaving
4
5 155 the solid sample in direct contact with the graphite tube wall. Under these conditions,
6
7 156 the temperature to which the analyte is subject is significantly higher than the actual
8
9 157 temperature of a graphite platform under the same nominal temperature,¹⁷ leading to
10
11 158 enhanced atomization efficiency for refractory elements.

12
13
14 159 Actually, the dynamic and static (final) temperatures of tube wall and platform
15
16 160 during an atomization cycle were only measured accurately for a transversely heated
17
18 161 graphite tube with integrated platform;¹⁷ however the results allow some extrapolation
19
20 162 also for a SS platform, which has a significantly greater mass. The graphite tube wall
21
22 163 was shown to heat very rapidly with some “overshooting” over the set temperature
23
24 164 when high heating rates are applied.¹⁷ This effect might be very beneficial when
25
26 165 refractory elements are atomized from the tube wall. Platforms don’t show this effect, as
27
28 166 they are heated by radiation from the tube wall, which causes a delay in the onset of
29
30 167 heating and a somewhat lower final temperature, the magnitude of both depends on the
31
32 168 mass of the platform used. This “platform effect” is beneficial for the determination of
33
34 169 volatile elements, and an essential part of the STPF concept.¹⁸ For the most refractory
35
36 170 elements, however, this effect results in increased tailing of the absorption signal and
37
38 171 memory effects.

39
40
41
42
43 172 Ideally, the TPS film should be easy to manipulate, so that it can be cut into the
44
45 173 desired platform-like shape, and it should be sufficiently resistant to allow grapping by
46
47 174 the pair of tweezers used to insert the platform into the graphite furnace. Considering
48
49 175 these aspects, TPS films produced using a Petri dish with a diameter of 9 cm formed
50
51 176 from 1.0 g of starch and 0.3 g sorbitol were selected for further experiments.

52
53
54
55
56 177 *3.2 Optimization of temperature program for degradation of the TPS platforms*
57
58
59
60

1
2
3 178 The thermal degradation of TPS film platforms was evaluated during the drying and
4
5 179 first pyrolysis stage by inserting a small mass of film (about 0.02 mg) into the graphite
6
7 180 tube and monitoring its disintegration with the internal camera available in the contrAA
8
9 181 instrument. Complete degradation of the film was observed at temperatures above 500
10
11 182 °C, within 20 s. Adoption of this ‘pre-pyrolysis’ stage led to a smooth disintegration of
12
13 183 the film, resulting in deposition of the solid sample directly onto the inner graphite tube
14
15 184 wall.

185 3.3. Temperature program optimization for aqueous solutions and solid samples

186 Molybdenum and V are thermally highly stable elements, which eliminates the need
187 to carry out individual optimization of pyrolysis temperatures for CRM and aqueous
188 solutions. Pyrolysis temperatures were selected based on previously published
189 procedures aiming at Mo and V determination available in the current literature,^{19,20} and
190 set as 1200 °C and 1100 °C for Mo and V, respectively.

191 Fig. 2 shows the atomization curves for Mo and V in aqueous solution; the highest
192 sensitivity was found using 2650 °C for Mo and 2600 °C for V, respectively; however,
193 in the case of Mo the optimum atomization temperature might even be higher than 2650
194 °C, but this is the maximum temperature that can be selected in the equipment used in
195 this work.

196 In the same way, the behavior of Mo and V was evaluated using a solid CRM
197 weighed onto a TPS platform. The corresponding atomization curves are shown in Figs.
198 3A and 3B. Approximately 0.07 mg of NIST SRM 1649a (\approx 1.0 ng Mo) and around 0.7
199 mg of CRM IAEA 336 (\approx 1.0 ng V), were weighed onto TPS platforms and submitted
200 to the temperature program. The atomization curves for the aqueous standard solutions

1
2
3 201 and the solid CRM are very similar, with optimum atomization temperatures of 2650 °C
4
5 202 for Mo and 2600 °C for V, respectively.
6

7 203 In the case of V (Fig. 3B), the maximum sensitivity is obtained at 2600 °C, and in the
8
9 204 case of Mo the optimum atomization temperature is only slightly higher. These high
10
11 205 temperatures are due to the carbides and oxides of V and Mo which have high
12
13 206 stability.¹¹ The atomization temperatures selected for the next optimizations were 2650
14
15 207 °C for Mo and 2600 °C for V.
16
17
18
19

20 208 *3.4. Comparison between TPS film and conventional graphite platform*

21
22

23 209 The next step was to compare the behavior of Mo and V in direct contact with the
24
25 210 tube wall after introduction on a TPS film as a sample holder and a conventional SS
26
27 211 graphite platform. Approximately 0.07 mg of the CRM NIST 1649a (≈ 1 ng Mo) was
28
29 212 weighed onto the TPS film and onto a graphite platform, respectively, using 15 s of hold
30
31 213 time for atomization in both cases. Fig. 4A shows the superimposed absorbance signals
32
33 214 for the two platform types, while Figs. 4B and 4C show the time-resolved absorbance
34
35 215 spectra around the 313.259 nm Mo line. Obviously, a much longer atomization time
36
37 216 would have been required for the atomization signal to return to the baseline,
38
39 217 particularly in the case of the graphite platform; however, the maximum time that can
40
41 218 be used at a temperature of 2650 °C is 15 s. Nevertheless, due to the higher temperature
42
43 219 of the tube wall, compared to the platform surface,¹⁷ Mo is atomized with greater
44
45 220 efficiency and with less tailing when introduced on the TPS platform.
46
47
48
49

50 221 There appears another strong absorption line within the spectral range covered by the
51
52 222 detector, which is due to Ni (313.410 nm). This is not a problem, as the two lines are
53
54 223 well separated due to the high resolution of the monochromator.
55
56
57
58
59
60

1
2
3 224 Similar results were found for V when the samples were introduced into the graphite
4
5 225 furnace on TPS film or on a conventional graphite platform (Figs. 5A, 5B and 5C).
6
7 226 Approximately 0.7 mg of CRM IAEA-336 (≈ 1 ng V) was accurately weighed onto the
8
9 227 platforms, and an atomization (hold) time of 20 s at 2600 °C was used. Fig. 5A shows
10
11 228 that, when the TPS film is used for sample introduction, atomization starts after about 1
12
13 229 s, the signal reaches a maximum after about 4 s and returns almost to the baseline after
14
15 230 about 15 s. In contrast, when the conventional SS graphite platform is used, atomization
16
17 231 only starts after about 3 s, the maximum is reached after 5-6 s with a much lower
18
19 232 maximum absorbance, and the signal does not return to the baseline within the 20 s of
20
21 233 atomization time. This is an important fact, since, as in the case of Mo, the lifetime of
22
23 234 the tube can be increased using TPS film by reducing the atomization time. Another
24
25 235 important point is the repeatability of the analytical signal using the TPS film, which
26
27 236 was much better when compared to the conventional graphite platform. This can be
28
29 237 explained by the faster atomization of the analyte during the first seconds in case of the
30
31 238 TPS film, where the gas phase temperature is higher due the absence of a graphite
32
33 239 platform, and the less pronounced tailing.

34
35
36
37
38 240 As in the case of Mo, different absorption lines can be seen in Figs. 5B and 5C in the
39
40 241 vicinity of the main analytical line of V. Firstly, there are the two additional lines of the
41
42 242 vanadium triplet at 318.342 and 318.541 nm, and there is also a strong Fe absorption at
43
44 243 318.48 nm.

45 46 47 48 49 244 *3.5. Comparison of direct SS analysis using TPS film and aqueous standard solutions*

50
51
52 245 The great perspective of using direct SS analysis with GF AAS is the possibility of
53
54 246 using aqueous standard solutions for calibration. In order to check this possibility in the
55
56 247 present case, aqueous solutions with an analyte mass of 0.3 ng Mo and 1.3 ng V,
57
58
59
60

1
2
3 248 respectively, were injected directly into the graphite tube onto the tube wall.
4
5 249 Approximately the same analyte mass in the form of solid samples was introduced via
6
7 250 the TPS platform and submitted to the temperature program in Table 1. The results that
8
9 251 are presented in Figs. 6 and 7 show that essentially the same integrated absorbance was
10
11 252 obtained in the case of Mo and that the signals were practically identical in the case of
12
13
14 253 V, respectively, indicating that aqueous standard solutions could be used for calibration.
15
16
17
18
19

20
21
22
23
24
25
26
27
28
29
30
31
32
33
34
35
36
37
38
39
40
41
42
43
44
45
46
47
48
49
50
51
52
53
54
55
56
57
58
59
60

255 3.6. Calibration and figures of merit

256 In the proposed method, TPS film platforms were used for direct SS analysis for Mo
257 and V determination using aqueous standard solutions for calibration. The linear
258 working range was from 0.09 to 5 ng Mo and from 0.5 to 20 ng V, respectively, with a
259 linear correlation better than $R = 0.998$. The limit of detection (LoD) was calculated as
260 $3 \sigma/S$ ($n = 10$), where σ is the standard deviation of 10 blank measurements and S is the
261 slope of the calibration curve. The LoD found for Mo and V using the proposed method
262 was 0.025 ng Mo and 0.13 ng V, respectively, while the characteristic mass, m_0 , was 7
263 pg for Mo and 18 pg for V, respectively. The figures of merit are summarized in Table
264 3.

265 It was essentially impossible, particularly in the case of Mo, to calculate figures of
266 merit for the graphite platform for comparison. The rapid deterioration of the graphite
267 tube and platform did not allow making a series of measurements for statistical
268 evaluation of the data. Fig. 8 shows an example for that problem; a quantity of about
269 0.22 mg of NIST SRM 1649a “Urban dust” has been analyzed eight times in sequence,
270 in both cases starting with a new graphite tube. The graphite platform was new as well
271 at the beginning of the experiment, but used for all the eight atomization cycles. A new

1
2
3 272 TPS platform had obviously to be used for each of the atomizations. Fig. 8 shows the
4
5 273 atomization signals that were obtained for the eighth measurement for each of the
6
7 274 platforms, which should be compared with those shown in Fig. 4A. The latter ones are
8
9 275 the first shot with a new tube and a new platform, the only difference being the sample
10
11 276 mass, which was more than three times higher in Fig. 8. It is obvious that the
12
13 277 atomization signal with the TPS platform remained essentially the same, whereas the
14
15 278 one with the graphite platform underwent a significant change. Actually, the absorbance
16
17 279 signal with the latter one changed with each atomization cycle, making any quantitative
18
19 280 evaluation impossible. The results obtained with the graphite platform for V were
20
21 281 clearly better than those for Mo; however, those obtained with the TPS platform were
22
23 282 still much better, so that no quantitative comparison has been made.
24
25
26
27
28

29 283 *3.7. Determination of Mo and V in CRM by HR-CS SS-GF AAS using TPS film*

30
31
32 284 The results of the determination of Mo in four CRMs, NIST 1577b (bovine liver),
33
34 285 NCS ZC 71001 (beef liver), NIST 1568a (rice flour), and NIST 1649a (urban dust)
35
36 286 using HR-CS SS-GF AAS and TPS film for sample introduction are shown in Table 4.
37
38 287 The results of the determination of V in CRM BCR 180 (gas coal), NIST 1648a (urban
39
40 288 particulate matter) and NIST 1649a using the same technique are shown in Table 5.

41
42
43 289 In all determinations the found values were in agreement with the certified ones at a
44
45 290 95% confidence interval (student t-test, $p > 0.05$), with relative standard deviations
46
47 291 (RSD) better than 8%. This shows that HR-CS SS-GF AAS using the new approach of
48
49 292 sample introduction on a TPS film and calibration against aqueous standard solutions
50
51 293 can be used for this kind of analysis.
52
53
54
55

56 294 **4. Conclusions**

1
2
3 295 One of the most beneficial results of using a TPS film for direct SS introduction for
4
5 296 GF AAS was the lifetime of the graphite tubes, which increased very significantly
6
7 297 compared to the use of conventional graphite platforms. This is mostly due to the
8
9 298 reduced tailing of the absorbance signals, which directly results in a reduction of the
10
11 299 atomization time. This is an important point because it is directly related to the cost of
12
13 300 analysis. Another important point is that the RSDs found in all determinations were
14
15 301 very low for direct SS analysis, demonstrating the repeatability of analytical signals
16
17 302 even for complex samples, such as coal and biological materials. The possibility of
18
19 303 using aqueous standard solutions for calibration further enhances the attractiveness of
20
21 304 the approach. It might be expected that the use of starch platforms for direct SS-GF
22
23 305 AAS analysis could be extended to the determination of other refractory elements in the
24
25 306 future.

307 **Acknowledgments**

308 The authors are grateful to the Conselho Nacional de Desenvolvimento Científico
309 and Tecnológico (CNPq), the Instituto Nacional de Ciência e Tecnologia do CNPq –
310 INCT de Energia e Ambiente, Salvador, BA, Brazil, and Coordenação de
311 Aperfeiçoamento de Pessoal de Nível Superior (CAPES) for financial support and
312 scholarships. The authors are also grateful to Analytik Jena for financial support and
313 donation of the contrAA 600 high-resolution continuum source atomic absorption
314 spectrometer. The authors also appreciate the help of Dr^a Maria da Graça Nascimento,
315 Universidade Federal de Santa Catarina (UFSC Brazil), for assistance in the
316 development and preparation of the starch films.

317 **References**

- 318 1 L. Jorhem, *Microchim. Acta* 1995, **119**, 211.
- 319 2 R.J. Warren, J.F. Hazel, W.M. McNabb, *Anal. Chim. Acta* 1959, **21**, 224.
- 320 3 H. Hashitani, H. Yoshida, T. Adachi, *Anal. Chim. Acta* 1975, **76**, 85.
- 321 4 N. Khan, I.S. Jeong, I.M. Hwang, J.S. Kim, S.H. Choi, E.Y. Nho, J.Y. Choi, B.-
322 M. Kwak, J.-H. Ahn, T. Yoon, K.S. Kim, *Food Chem.* 2013, **141**, 3566.
- 323 5 E. Vassileva, H. Dočekalová, H. Baeten, S. Vanhentenrijk, M. Hoenig, *Talanta*
324 2001, **54**, 187.
- 325 6 J.A. Nóbrega, M.C. Santos, R.A. de Sousa, S. Cadore, R.M. Barnes, M. Tatro,
326 *Spectrochim. Acta, Part B* 2006, **61**, 465.
- 327 7 B. Welz, M.G.R. Vale, D.L.G. Borges, U. Heitmann, *Anal. Bioanal.Chem.* 2007,
328 **389**, 2085.
- 329 8 É.R. Pereira, I.N.B. Castilho, B. Welz, J.S. Gois, D.L.G. Borges, E. Carasek,
330 J.B. de Andrade, *Spectrochim. Acta, Part B* 2014, **96**, 33.
- 331 9 K.W. Jackson, *Electrothermal atomization for analytical atomic spectrometry*,
332 John Wiley & Sons Ltd, Chichester, 1999, p. 470.
- 333 10 R. Nowka, I.L. Marr, T.M. Ansari, H. Muller, *Fresenius J. Anal. Chem.* 1999,
334 **364**, 533.
- 335 11 B. Welz, M. Sperling, *Atomic Absorption Spectrometry*, third ed. Wiley-VCH,
336 Weinheim, 1999.
- 337 12 H. Liu, F. Xie, L. Yu, L. Chen, L. Li, *Prog. Polym. Sci.* 2009, **34**, 1348.
- 338 13 R.F. Tester, J. Karkalas, X. Qi, *J. Cereal Sci.* 2004, **39**, 151.
- 339 14 A.L.D. Róz, A.J.F. Carvalho, A. Gandini, A.A.S. Curvelo, *Carbohydr. Polym.*
340 2006, **63**, 417.
- 341 15 Y.P. Chang, A. Abd Karim, C.C. Seow, *Food Hydrocolloid* 2006, **20**, 1.

- 1
2
3 342 16 I.G. Donhowe, O.R. Fennema, Edible films and coatings: characteristics,
4
5 343 formation, definitions and testing methods. Lancaster, PA (USA): Technomic
6
7 344 Publishing Co., 1994, p.25.
8
9 345 17 M. Sperling, B. Welz, J. Hertzberg, C. Rieck, G. Marowsky, *Spectrochim. Acta*,
10
11 346 *Part B* 1996, **51**, 897.
12
13 347 18 W. Slavin, D.C. Manning, G.R. Carnrick, *At. Spectrom.* 1981, **2**, 137.
14
15 348 19 I.N.B. Castilho, B. Welz, M.G.R. Vale, J.B. de Andrade, P. Smichowski, A.A.
16
17 349 Shaltout, L. Colares, E. Carasek, *Talanta* 2012, **88**, 689.
18
19 350 20 M.M. Silva, I.C.F. Damin, M.G.R. Vale, B. Welz, *Talanta* 2007, **71**, 1877.
20
21
22
23 351
24
25
26
27
28
29
30
31
32
33
34
35
36
37
38
39
40
41
42
43
44
45
46
47
48
49
50
51
52
53
54
55
56
57
58
59
60

352 Table 1. Temperature program adopted for Mo and V determination using HR-CS SS-
 353 GF AAS.

Stage	Temperature / °C	Ramp / °C s ⁻¹	Hold / s	Ar gas flow-rate / L min ⁻¹
Drying 1	110	6	15	0.3
Drying 2	160	5	15	0.3
Pyrolysis 1	510	10	20	0.3
Pyrolysis 2	1200 ^a ; 1100 ^b	50	10	2.0
Atomization	2650 ^a ; 2600 ^b	FP ^c	15 ^a ; 20 ^b	0
Cleaning	2650	0 ^a ; 150 ^b	4	2.0

354 ^a molybdenum ^b vanadium ^c FP = Full power

355

356

357 Table 2. Combined conditions adopted to evaluate the characteristics of the TPS film
 358 used for HR-CS SS-GF AAS analysis.

Experiment	Starch mass / g	Plasticizer type	Plasticizer mass / g	Petri dish diameter / cm
1	1.0	sorbitol	0.3	7.5
2	1.0	sorbitol	0.3	9.5
3	0.5	sorbitol	0.1	9.5
4	0.5	glycerol	0.1	9.5
5	1.0	sorbitol	0.1	9.5

359

360

361 Table 3. Figures of merit for the determination of Mo and V using HR-CS SS-GF AAS
 362 and TPS film for direct SS analysis with calibration against aqueous standards.

Parameters	Mo	V
Limit of detection, pg	25	130
Characteristic mass, pg	7	18
Correlation coefficient, R	0.999	0.998
Linear working range, ng	0.09 - 0.50	0.5 - 20

363

364

365

366 Table 4. Molybdenum determination in different CRMs by HR-CS SS-GF AAS with
 367 TPS film for SS introduction and aqueous standard solutions for calibration. The values
 368 represent the mean of three measurements \pm SD.

CRM	Found / $\mu\text{g g}^{-1}$	Certified / $\mu\text{g g}^{-1}$	RSD / %
NIST 1577b	3.6 ± 0.1	3.5 ± 0.3	3
NIST 1568a	1.6 ± 0.1	1.46 ± 0.08	6
NCS ZC 71001	3.5 ± 0.3	3.76 ± 0.3	8
NIST 1649a	13.9 ± 0.5	13.5 ± 0.9	3

369

370

371

1
2
3
4 372 Table 5. Vanadium determination in different CRMs by HR-CS SS-GF AAS with TPS
5
6 373 film for SS introduction and aqueous standard solutions for calibration. The values
7
8
9 374 represent the mean of three measurements \pm SD.

CRM	Found / $\mu\text{g g}^{-1}$	Certified / $\mu\text{g g}^{-1}$	RSD / %
NIST 1649a	336 ± 24	345 ± 13	7
NIST 1648a	132 ± 2	127 ± 11	1
BCR 180	21 ± 1	19 ± 1	7

10
11
12
13
14
15
16
17
18
19 375

20
21 376

22
23 377

24
25
26 378
27
28
29
30
31
32
33
34
35
36
37
38
39
40
41
42
43
44
45
46
47
48
49
50
51
52
53
54
55
56
57
58
59
60

1
2
3 379 **Figure captions**
4
5

6 380 Fig. 1. Introduction of (A) the TPS platform and (B) the graphite platform using the
7
8 381 manual SS accessory; (C) and (D) show the position of the TPS platform inside the
9
10 382 graphite tube; picture taken with the video camera of the contra 600; (C) empty TPS
11
12 383 platform, (D) TPS platform with solid sample.
13
14

15
16 384 Fig. 2. Atomization curves for 0.4 ng Mo (■) and 1.0 ng V (▲) in aqueous standard
17
18 385 solution. Pyrolysis temperature was fixed at 1200 °C for Mo and 1100 °C for V.
19
20

21 386 Fig. 3. Atomization curves for: (A) Mo – about 0.07 mg of CRM NIST 1649a (≈ 1 ng of
22
23 387 Mo); and (B) V – about 0.7 mg of CRM IAEA 336 (≈ 1 ng of V) on the TPS platform.
24
25 388 All integrated absorbance values normalized for 1 mg of sample weight. Pyrolysis
26
27 389 temperature of 1200 °C for Mo and 1100 °C for V.
28
29

30
31 390 Fig. 4. Comparison of absorbance signals for about 0.07 mg of CRM NIST 1649a
32
33 391 (≈ 1 ng Mo), deposited on TPS film and graphite platform, respectively. (A)
34
35 392 Superimposed absorbance signals measured at the CP at 313.259 nm using a TPS film
36
37 393 (solid line) and a graphite platform (broken line). (B) and (C): time-resolved absorbance
38
39 394 spectra using: (B) TPS film and (C) conventional graphite platform; $T_{\text{PYR}} = 1200$ °C and
40
41 395 $T_{\text{AT}} = 2650$ °C.
42
43

44 396 Fig. 5. Comparison of absorbance signals for about 0.7 mg of CRM IAEA-336
45
46 397 (≈ 1 ng V), deposited on TPS film and graphite platform, respectively. (A)
47
48 398 Superimposed absorbance signals measured at the CP at 318.398 nm using a TPS film
49
50 399 (solid line) and a graphite platform (dotted line), respectively. (B) and (C): time-
51
52 400 resolved absorbance spectra using: (B) TPS film and (C) conventional graphite
53
54 401 platform; $T_{\text{PYR}} = 1100$ °C and $T_{\text{AT}} = 2600$ °C.
55
56
57
58
59
60

1
2
3 402 Fig. 6. Comparison of absorbance signals for approximately 0.3 ng Mo; solid line:
4
5 403 ≈ 0.02 mg of CRM NIST 1649a, introduced on a TPS film; broken line: 15 μL of
6
7 404 $20 \mu\text{g L}^{-1}$ Mo solution injected directly onto the tube wall. $T_{\text{Pyr}} = 1200 \text{ }^\circ\text{C}$ and $T_{\text{At}} =$
8
9 405 $2650 \text{ }^\circ\text{C}$.

10
11 406 Fig. 7. Comparison of absorbance signals for approximately 1.3 ng V; solid line:
12
13 407 ≈ 0.9 mg of CRM IAEA-336, introduced on a TPS film; broken line: 6.5 μL of 200 μg
14
15 408 L^{-1} V solution injected directly onto the tube wall. $T_{\text{Pyr}} = 1100 \text{ }^\circ\text{C}$ and $T_{\text{At}} = 2600 \text{ }^\circ\text{C}$.

16
17 409 Fig. 8. Comparison of absorbance signals for Mo in ≈ 0.22 mg of CRM NIST 1649a
18
19 410 after eight atomization cycles; solid line: TPS film platform; dotted line: graphite
20
21 411 platform; $T_{\text{Pyr}} = 1200 \text{ }^\circ\text{C}$ and $T_{\text{At}} = 2650 \text{ }^\circ\text{C}$. Both measurement cycles started with new
22
23 412 graphite tubes, and in the case of the graphite platform with a new platform.
24
25
26
27

28 413
29
30

31 414
32
33
34
35
36
37
38
39
40
41
42
43
44
45
46
47
48
49
50
51
52
53
54
55
56
57
58
59
60

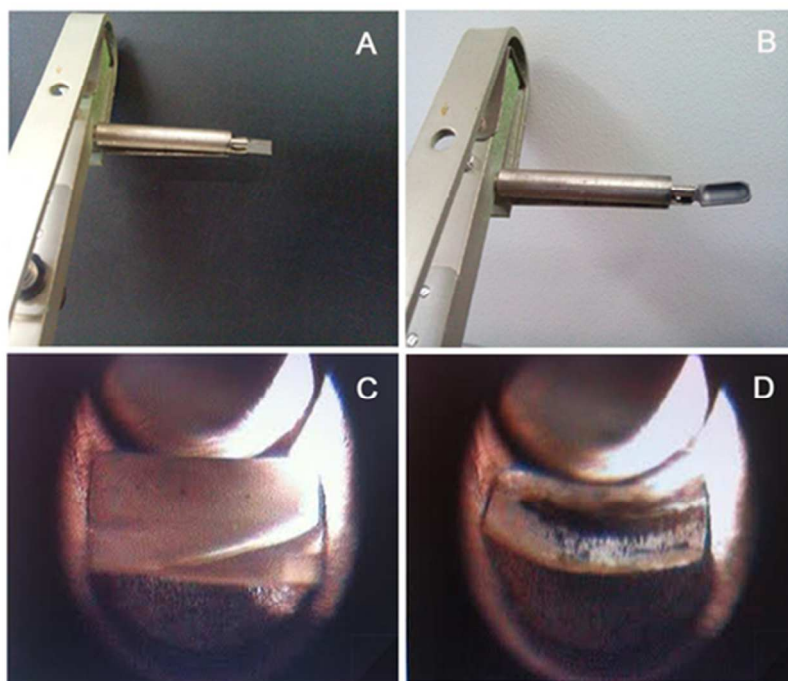


Fig. 1. Introduction of (A) the TPS platform and (B) the graphite platform using the manual SS accessory; (C) and (D) show the position of the TPS platform inside the graphite tube; picture taken with the video camera of the contra 600; (C) empty TPS platform, (D) TPS platform with solid sample.
50x36mm (300 x 300 DPI)

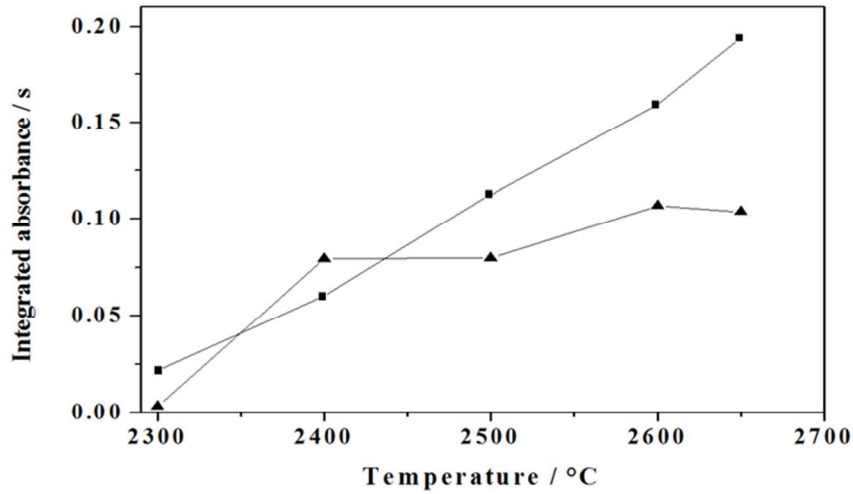
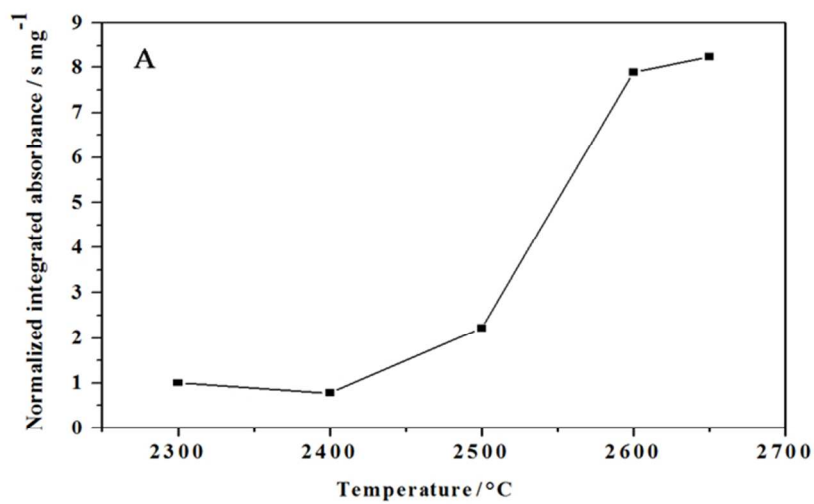


Fig. 2. Atomization curves for 0.4 ng Mo (v) and 1.0 ng V (▲) in aqueous standard solution. Pyrolysis temperature was fixed at 1200 °C for Mo and 1100 °C for V.
70x39mm (300 x 300 DPI)



70x39mm (300 x 300 DPI)

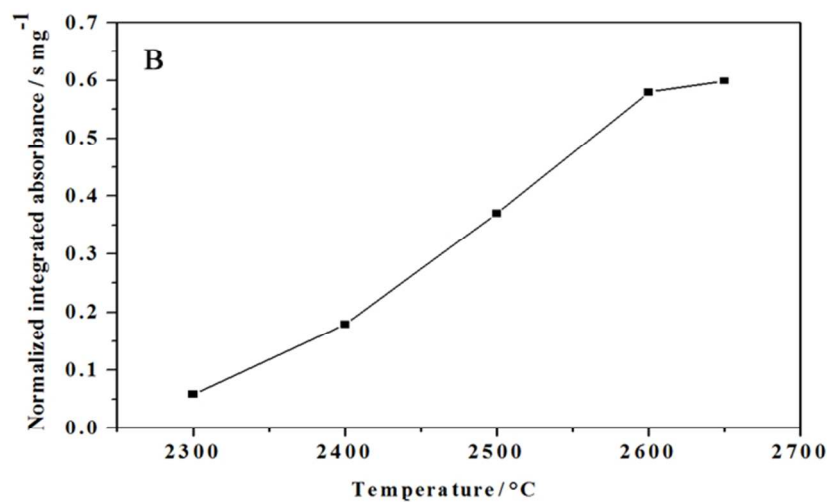
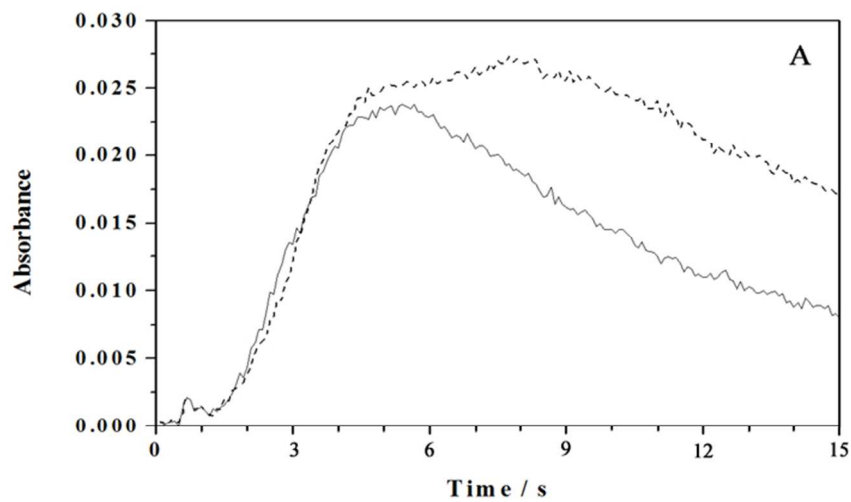
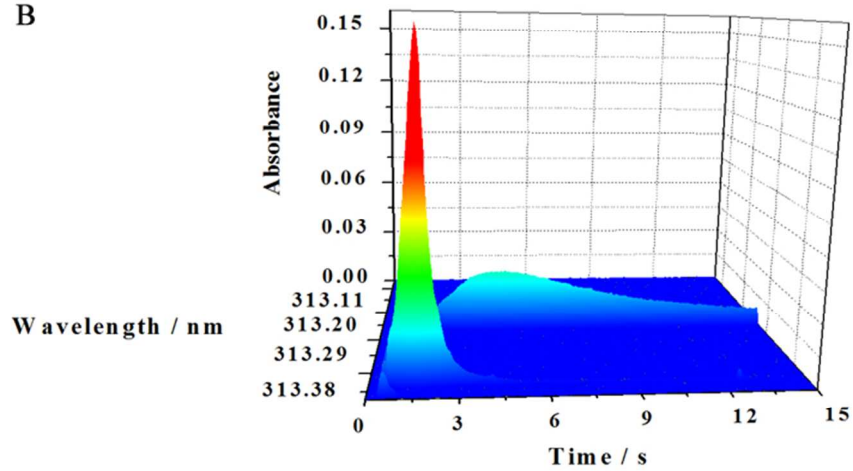


Fig. 3. Atomization curves for: (A) Mo – about 0.07 mg of CRM NIST 1649a (≈ 1 ng of Mo); and (B) V – about 0.7 mg of CRM IAEA 336 (≈ 1 ng of V) on the TPS platform. All integrated absorbance values normalized for 1 mg of sample weight. Pyrolysis temperature of 1200 °C for Mo and 1100 °C for V. 70x39mm (300 x 300 DPI)



70x39mm (300 x 300 DPI)

B



70x39mm (300 x 300 DPI)

1
2
3
4
5
6
7
8
9
10
11
12
13
14
15
16
17
18
19
20
21
22
23
24
25
26
27
28
29
30
31
32
33
34
35
36
37
38
39
40
41
42
43
44
45
46
47
48
49
50
51
52
53
54
55
56
57
58
59
60

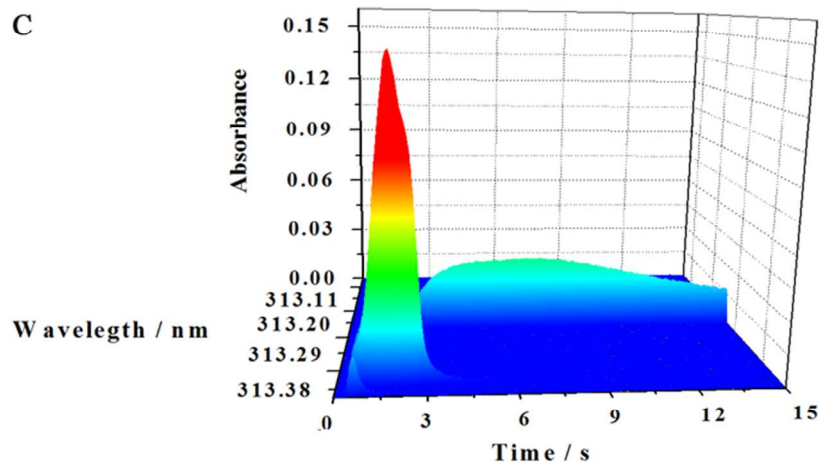
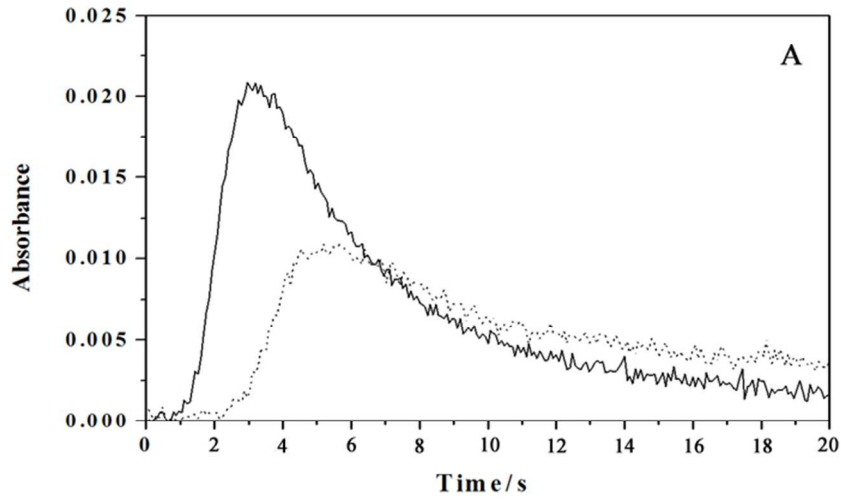


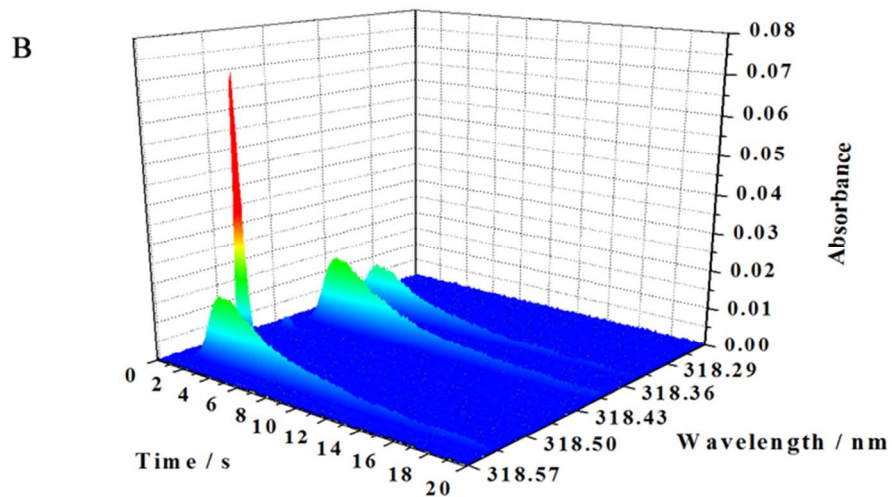
Fig. 4. Comparison of absorbance signals for about 0.07 mg of CRM NIST 1649a (≈ 1 ng Mo), deposited on TPS film and graphite platform, respectively. (A) Superimposed absorbance signals measured at the CP at 313.259 nm using a TPS film (solid line) and a graphite platform (broken line). (B) and (C): time-resolved absorbance spectra using: (B) TPS film and (C) conventional graphite platform; TPyr = 1200 °C and TAt = 2650 °C.

70x39mm (300 x 300 DPI)



70x39mm (300 x 300 DPI)

1
2
3
4
5
6
7
8
9
10
11
12
13
14
15
16
17
18
19
20
21
22
23
24
25
26
27
28
29
30
31
32
33
34
35
36
37
38
39
40
41
42
43
44
45
46
47
48
49
50
51
52
53
54
55
56
57
58
59
60



70x39mm (300 x 300 DPI)

1
2
3
4
5
6
7
8
9
10
11
12
13
14
15
16
17
18
19
20
21
22
23
24
25
26
27
28
29
30
31
32
33
34
35
36
37
38
39
40
41
42
43
44
45
46
47
48
49
50
51
52
53
54
55
56
57
58
59
60

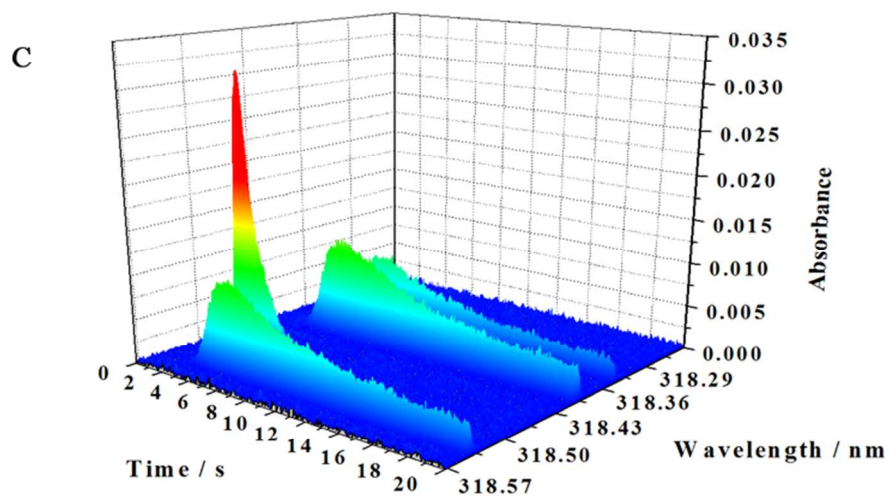


Fig. 5. Comparison of absorbance signals for about 0.7 mg of CRM IAEA-336 (≈ 1 ng V), deposited on TPS film and graphite platform, respectively. (A) Superimposed absorbance signals measured at the CP at 318.398 nm using a TPS film (solid line) and a graphite platform (dotted line), respectively. (B) and (C): time-resolved absorbance spectra using: (B) TPS film and (C) conventional graphite platform; $T_{Pyr} = 1100$ °C and $T_{At} = 2600$ °C.
70x39mm (300 x 300 DPI)

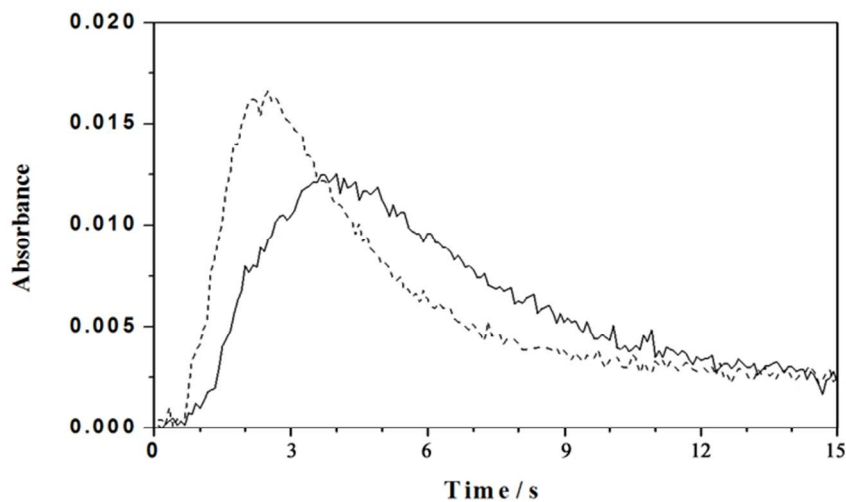


Fig. 6. Comparison of absorbance signals for approximately 0.3 ng Mo; solid line: ≈ 0.02 mg of CRM NIST 1649a, introduced on a TPS film; broken line: 15 μL of 20 $\mu\text{g L}^{-1}$ Mo solution injected directly onto the tube wall. TPyr = 1200 $^{\circ}\text{C}$ and TAt = 2650 $^{\circ}\text{C}$.

70x39mm (300 x 300 DPI)

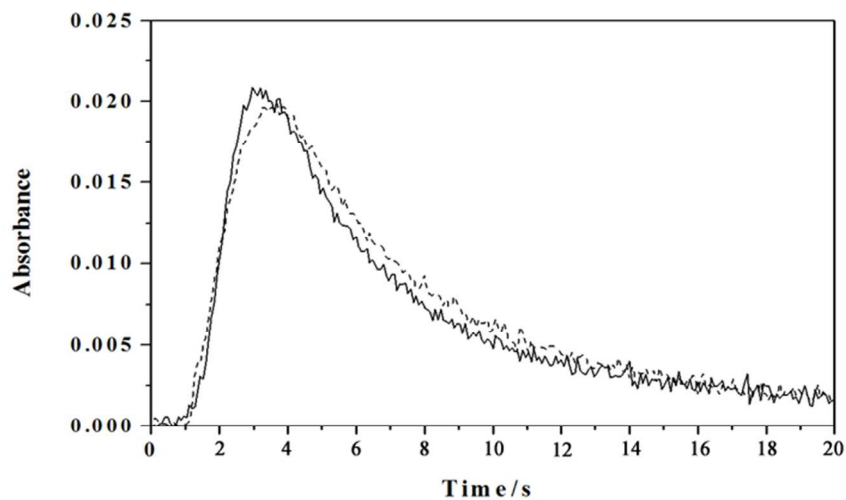


Fig. 7. Comparison of absorbance signals for approximately 1.3 ng V; solid line: ≈ 0.9 mg of CRM IAEA-336, introduced on a TPS film; broken line: 6.5 μL of 200 $\mu\text{g L}^{-1}$ V solution injected directly onto the tube wall. $T_{\text{Pyr}} = 1100$ $^{\circ}\text{C}$ and $T_{\text{At}} = 2600$ $^{\circ}\text{C}$.

70x39mm (300 x 300 DPI)

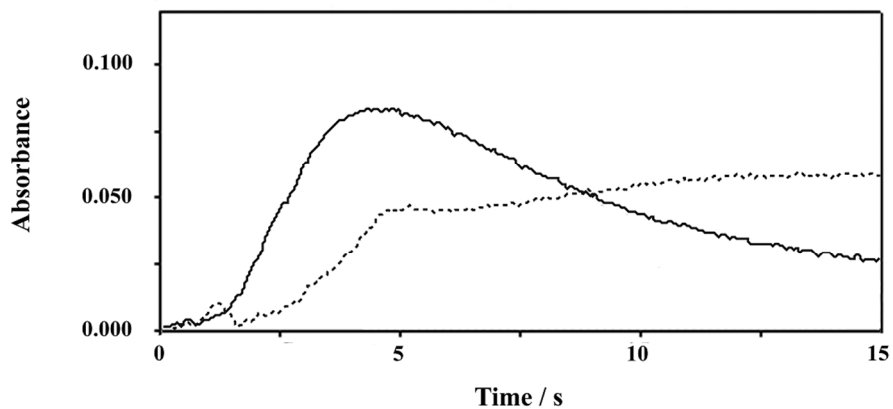


Fig. 8. Comparison of absorbance signals for Mo in ≈ 0.22 mg of CRM NIST 1649a after eight atomization cycles; solid line: TPS film platform; dotted line: graphite platform; $T_{Pyr} = 1200$ °C and $T_{At} = 2650$ °C. Both measurement cycles started with new graphite tubes, and in the case of the graphite platform with a new platform.
104x46mm (300 x 300 DPI)